Conformational rearrangement of gastric H^+,K^+-ATPase induced by an acid suppressant

Kazuhiro Abe, Kazutoshi Tani & Yoshinori Fujiyoshi

Department of Biophysics, Faculty of Science, Kyoto University, Kyoto, 606-0852, Japan

Supplementary Information

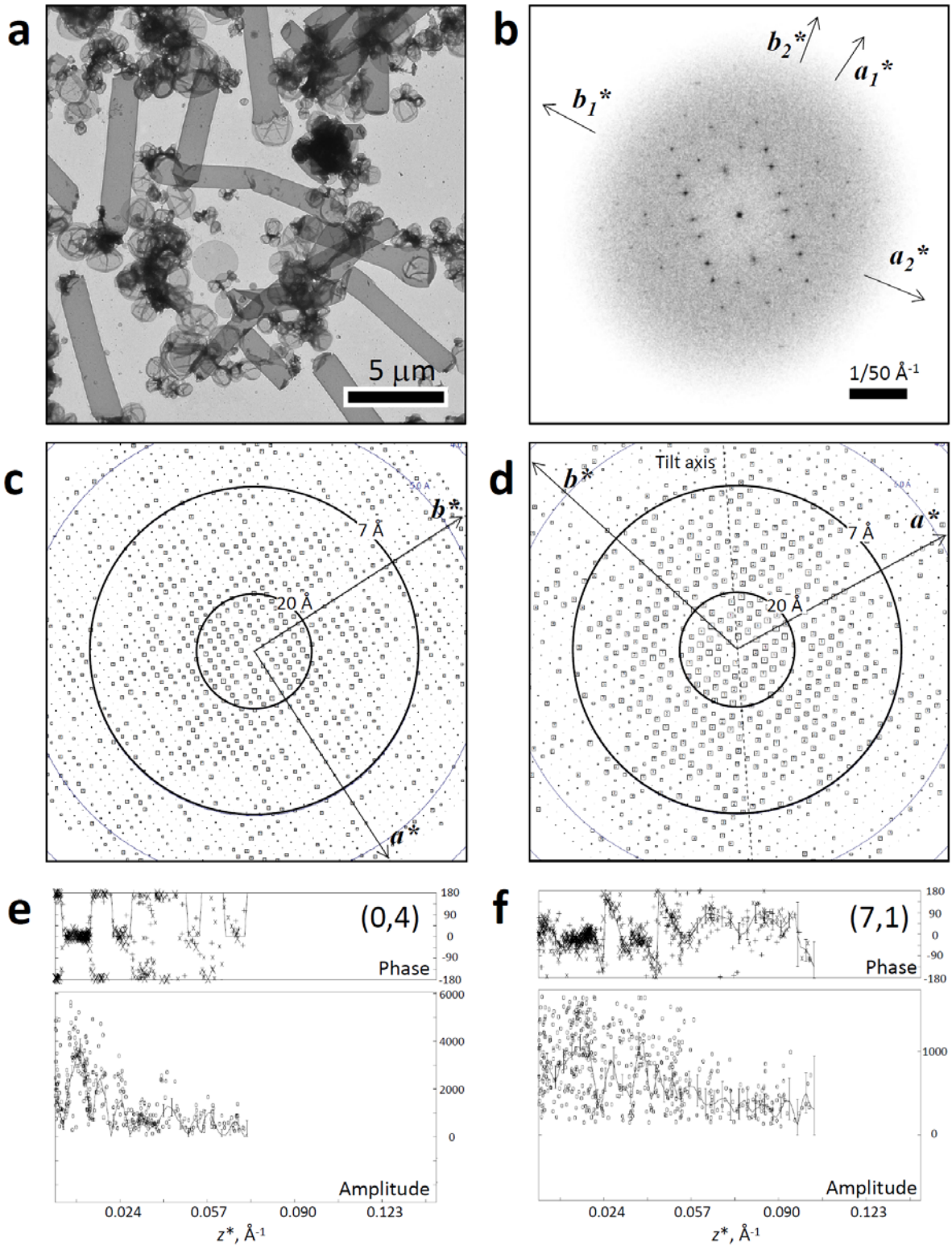

Supplementary Figure S1| **Two-dimensional crystals of (SCH)E_2BeF.** (a) Negatively stained tubular crystals. (b) The Fourier transform of negatively stained 2D crystal shows two overlapped lattices (a_1* b_1* and a_2* b_2*). (c) IQ-plot[47] calculated from a non-tilted image of a frozen-hydrated 2D crystal. (d) IQ-plot calculated from an image of a 45° tilted 2D crystal taken by the liquid helium-cooled cryo-electron microscope. (e,f) Representative lattice lines from the 3D data set. The phase (upper panel) and amplitude (lower panel) data of (0,4) lattice line (e) and those of the (7,1) lattice line (f).

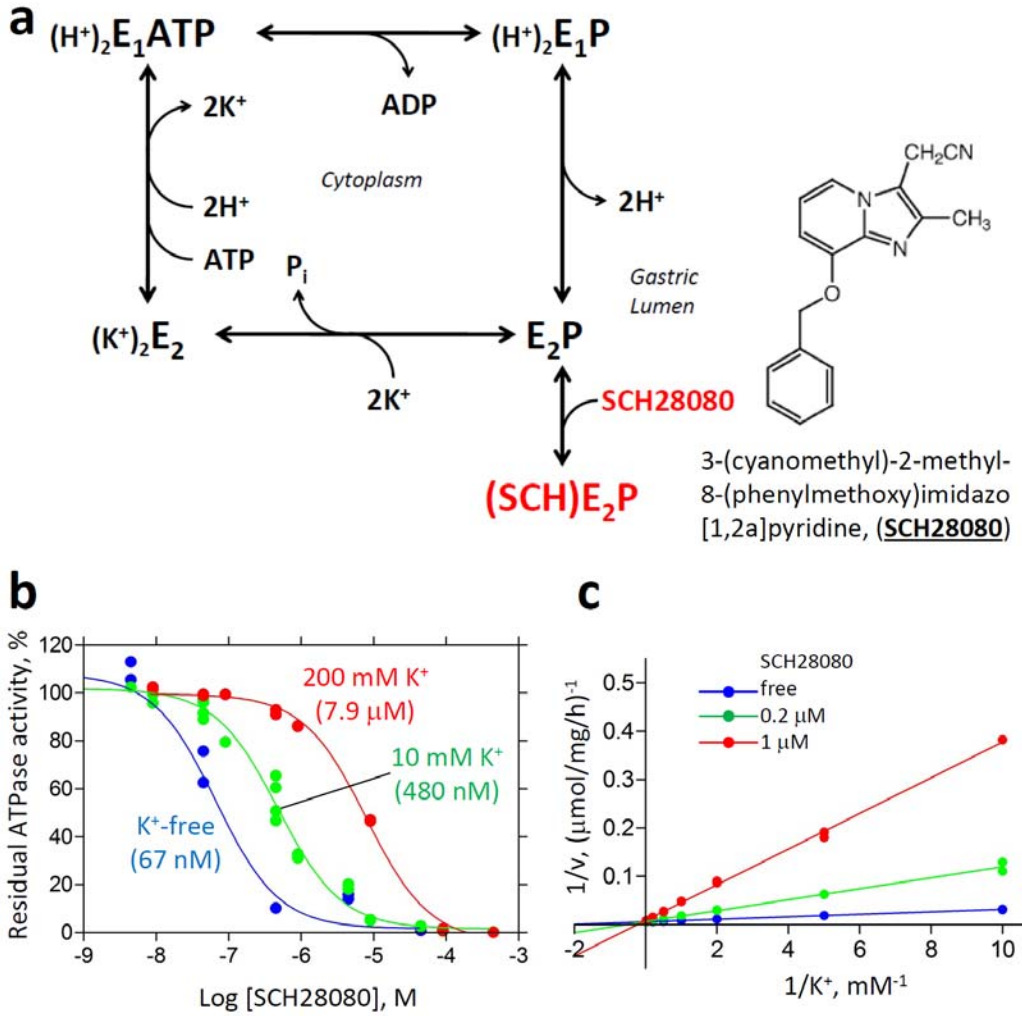

Supplementary Figure S2| **The transport cycle of gastric H^+,K^+-ATPase and its K^+-competitive antagonist.** (a) According to the Post-Albers-type reaction scheme, the cation transport and ATP hydrolysis are coupled to the cyclic conversion of the enzyme (abbreviates as "E") between E_1 and E_2, and their phosphorylated forms, E_1P and E_2P. Conformations of the enzyme that bind cations for outward transport (H^+) are defined as E_1, whereas those that bind luminal cation (K^+) are termed E_2. Proton binding to E_1 activates autophosphorylation from Mg^{2+}-ATP to form E_1P, which is soon converted to E_2P in the H^+-transporting step. Binding of K^+ to the E_2P form stimulates dephosphorylation and the transition to the occluded form $(K^+)E_2$. Subsequently, ATP-binding in a low-affinity mode accelerates a conformational change to E_1, and K^+ ions are released to the cytoplasm. The stoichiometry of hydrolyzed ATP and H^+/K^+ exchange is variable, from $2H^+/2K^+/1ATP$ at pH 6.1[48] to $1H^+/1K^+/1ATP$ at pH below 3.0[49]. SCH28080, a P-CAB prototype, preferentially binds to the E_2P conformation[16]. Because the 2D crystals formed in the presence of the phosphate analog and SCH28080, the present structure represents the E_2P conformation with bound SCH28080, $(SCH)E_2P$ (highlighted in red). (b,c) Inhibition of H^+,K^+-ATPase activity by SCH28080. Each measured value, which was obtained from 2 to 4 independent experiments using different membrane fraction lots, were plotted. (b) Dose-dependent inhibition of H^+,K^+-ATPase activity by SCH28080 in the presence or absence of K^+. The concentrations required for the half inhibition (IC_{50}) are indicated in the figure, showing K^+-dependent decrease in SCH28080-affinity. The IC_{50} in the absence of K^+ (67 nM) is consistent with the previously reported K_d for SCH28080-binding to the E_2P conformation (47 nM in ref 16). (c) Inverse plot of $1/v$ vs $1/[K^+]$ in the presence or absence of SCH28080, showing K^+-competitive inhibition of SCH28080. The ATPase activities were measured according to the method described in ref. 4.

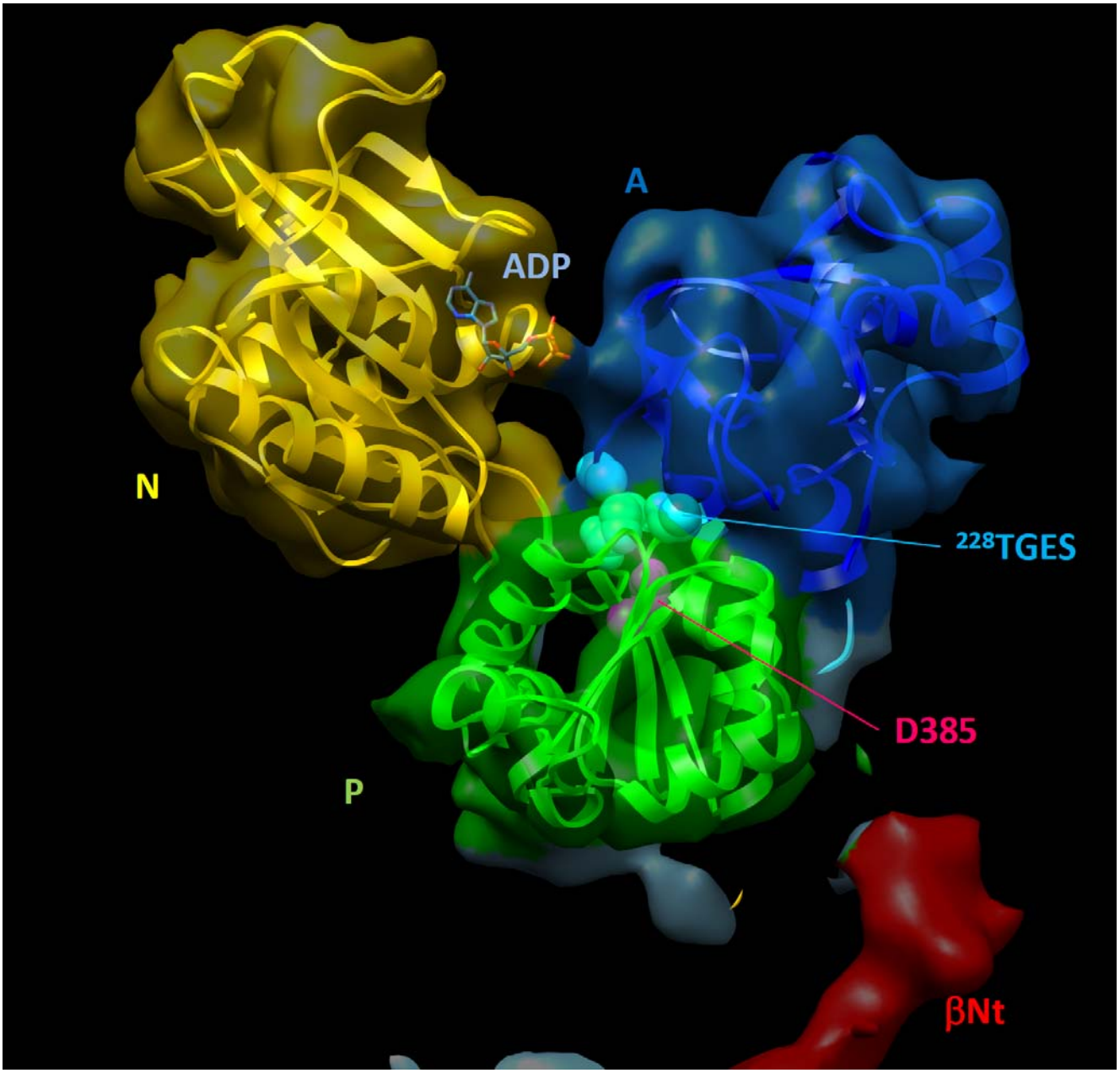

Supplementary Figure S3| **Cytoplasmic domains of the H^+,K^+-ATPase (SCH)E_2BeF conformation.** EM density map of (SCH)E_2BeF is shown as surface (1σ contour level) with superimposed homology model (ribbon). Color codes as in Fig. 1a. Cyan and magenta spheres indicate the TGES-motif and phosphorylated aspartate residue, respectively.

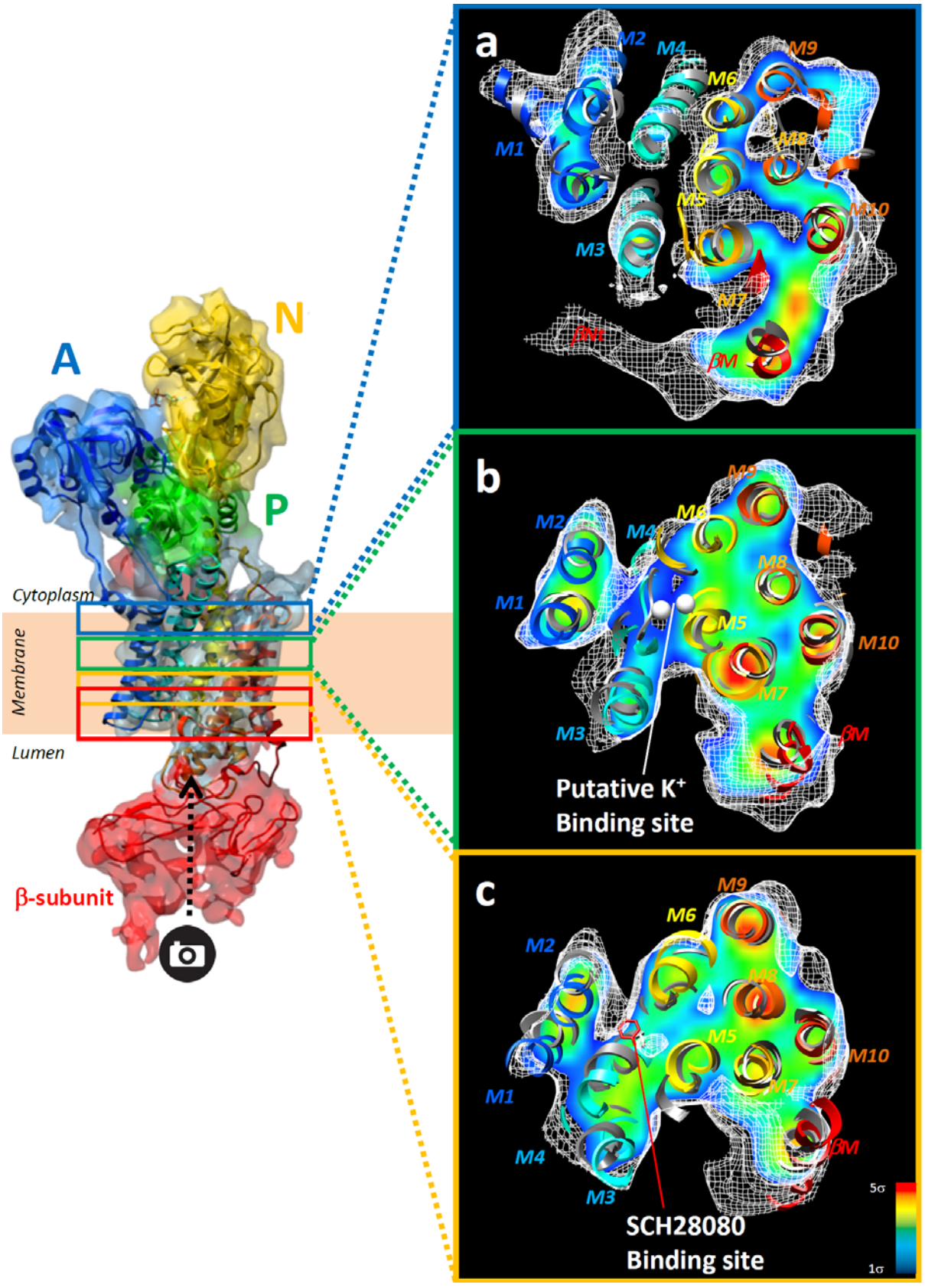

Supplementary Figure S4| **Horizontal sections of the TM region viewed from the luminal side of the membrane.** The positions for each section are indicated as colored boxes in the whole structure (left). The red box indicates the position for the slice displayed in Fig. 3a. Color codes as in Fig. 3a.

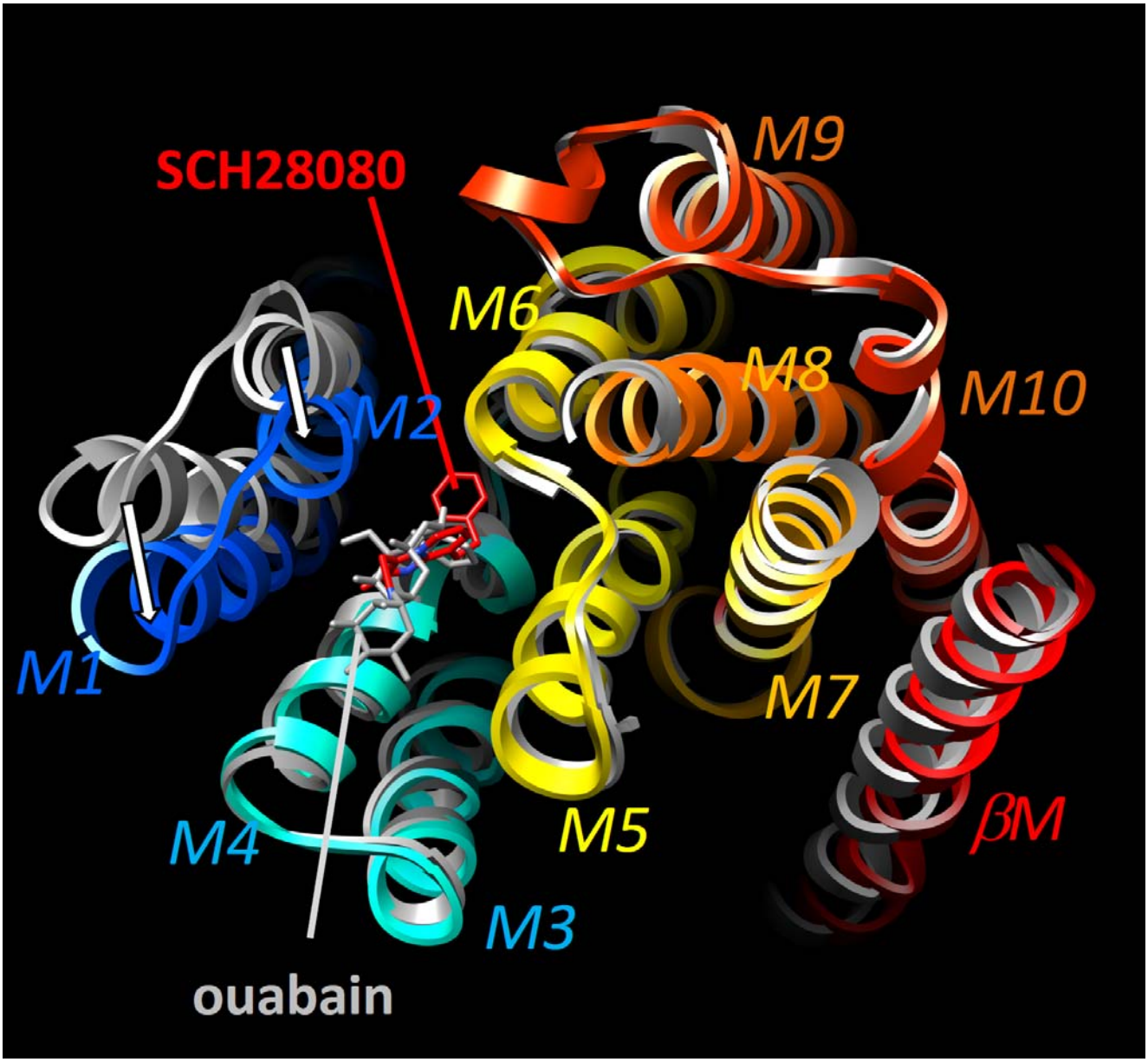

Supplementary Figure S5| **Comparison of the TM helices between SCH28080-bound H^+,K^+-ATPase and ouabain-bound Na^+,K^+-ATPase.** TM helices of H^+,K^+-ATPase $(SCH)E_2BeF$ structure are shown as color ribbons (as in Fig. 1a), and that of ouabain-bound Na^+,K^+-ATPase (PDB code 3A3Y) as grey ribbons. A cross-section of the luminal TM region parallel to the membrane plane is viewed from the luminal side of the membrane (as shown in Fig. 3). Bound SCH28080 and ouabain is shown as red and grey sticks, respectively. White arrows indicate the major conformational difference observed in the TM region of these structures (M1 and M2 shift 7.2Å and 8.8Å, respectively).

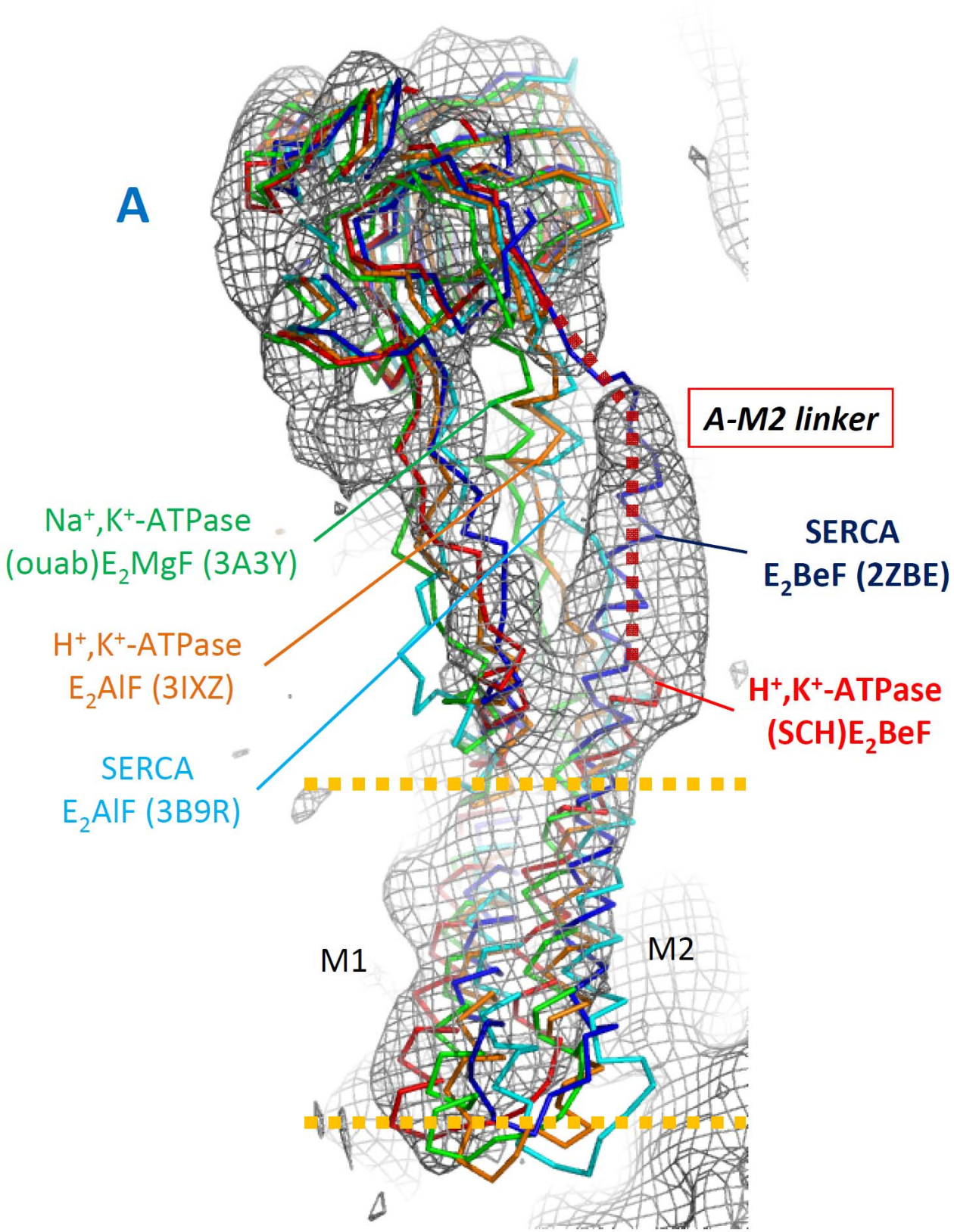

Supplementary Figure S6| **Comparison of the A-M2 linker conformation.** The grey mesh shows the EM density map of H^+,K^+-ATPase (SCH)E_2BeF with superimposed C^α traces of the several of known structures as indicated in the figure. Among them, the A-M2 linker of SERCA E_2BeF (blue) fits best into the closest conformation compared with the EM map of (SCH)E_2BeF.

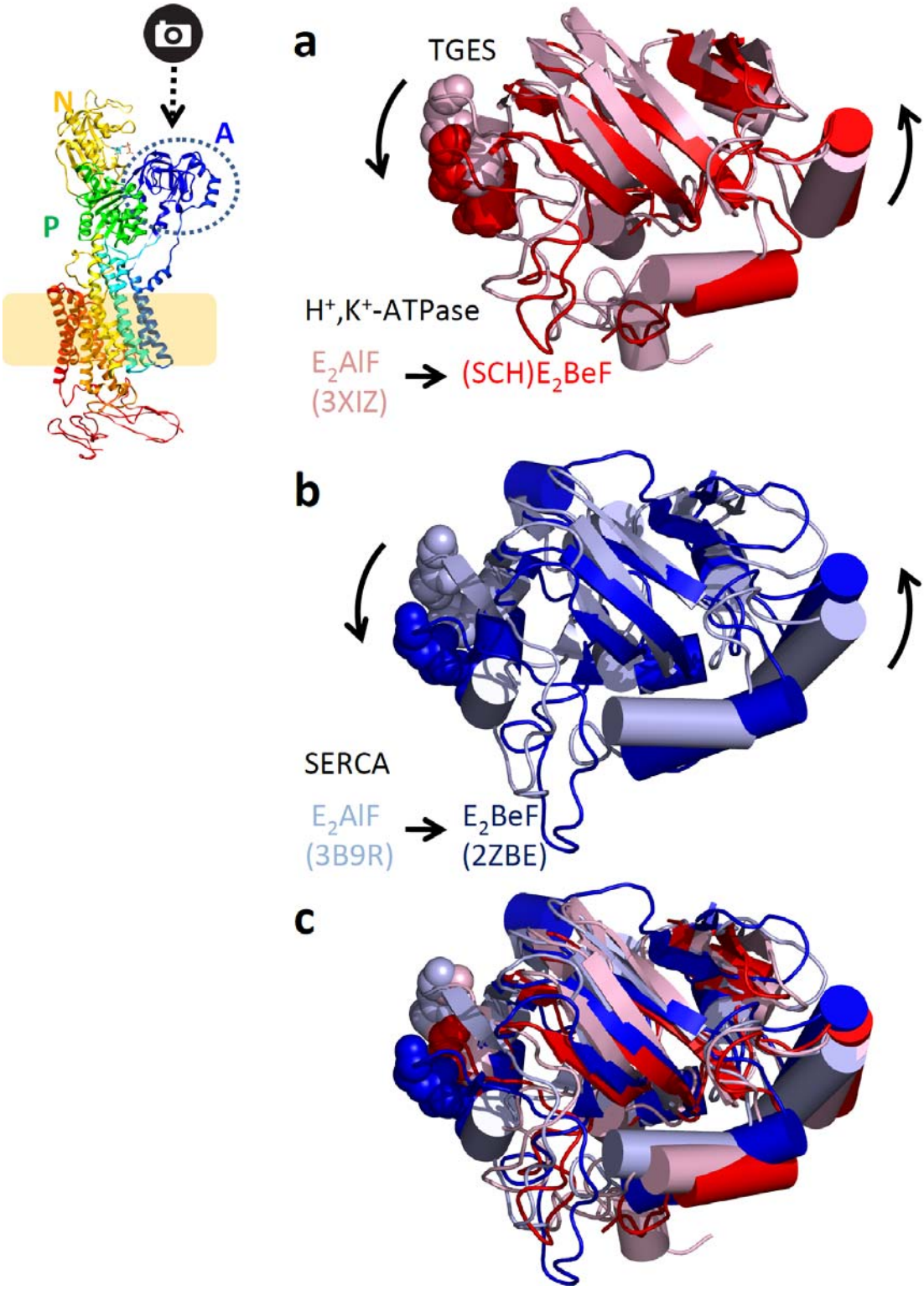

Supplementary Figure S7| **Rotation of the A domain.** Comparison of the azimuthal position of the A domain between the E_2AlF and $(SCH)E_2BeF$ homology models of H^+,K^+-ATPase (a), E_2AlF and E_2BeF structures of SERCA (b), or all of them (c). Only the A domains are shown as ribbon models, viewed from the cytoplasmic side of the molecules (as indicated on the left) with the highly conserved TGES-motif depicted as spheres for clarity. Black arrows indicate the rotational movement of the A domain during transition of two conformations as indicated in the figure.

Two-dimensional crystal		
	Space group	$p22_12_1$
	Lattice constants a = 140.9 Å, b = 111.3 Å, c = 320.0 Å (assumed), γ = 90.0°	
Electron micrographs		
	Approximate tilt angle	No. of images
	0°	7
	20°	87
	45°	222
	60°	199
	Total	515
Resolution limit		
	Parallel to the membrane plane	7.0 Å
	Perpendicular to the membrane plane	8.0 Å
Maximum tilt angle		64.0°
Range of underfocus		5,800 ~ 41,300 Å
Number of observed reflections		87,734 (5199)[a]
	unique reflections	6,801 (690)
Overall weighted phase residuals[b]		37.1° (63.4°)
Overall weighted R-factor[b]		0.4032 (0.329)

Supplementary Table S1| **Electron crystallographic data**

a. Values in parentheses refer to data in the highest resolution shell (7.3-7.0 Å).

b. 90° is random. Used reflections are ≤ IQ 6.

Supplementary references

47. Henderson, R., Baldwin, J., Downing, K., Lepault, J., & Zemiln, F. Structure of purple membrane from Halobacterium halobium: recording, measurement and evaluation of electron micrographs at 3.5Å resolution. *Ultramicroscopy* **19**, 147-178 (1986).

48. Reenstra, W. W. & Forte, J. G. H^+/ATP stoichiometry for the gastric (K^+ + H^+)-ATPase. *J. Membr. Biol.* **61**, 55-60 (1981).

49. Rabon, E. C., McFall, T. L. & Sachs, G. The gastric [H,K]ATPase: H^+/ATP stoichiometry. *J. Biol. Chem.* **257**, 6296-6299 (1982).